

PMPA for nephroprotection in PSMA-targeted radionuclide therapy of prostate cancer

Clemens Kratochwil (1), Frederik L. Giesel (1), Karin Leotta (2), Matthias Eder (3), Torsten Hoppe-Tichy (4), Hagop Youssoufian (5), Klaus Kopka (3), John W. Babich* (6), Uwe Haberkorn* (1, 2)

1. Department of Nuclear Medicine, University Hospital Heidelberg, Heidelberg, Germany
2. Clinical Cooperation Unit Nuclear Medicine, German Cancer Research Center (dkfz), Heidelberg, Germany
3. Division of Radiopharmaceutical Chemistry, German Cancer Research Center (dkfz), Heidelberg, Germany
4. Pharmacy Department, University Hospital of Heidelberg, Heidelberg, Germany
5. Progenics Pharmaceuticals Inc., Tarrytown NY, USA
6. Department of Radiopharmacy, Weill Cornell Medical College, New York NY, USA

* Senior authorship is equally shared by John W. Babich and Uwe Haberkorn

Corresponding author:

Dr. med. Clemens Kratochwil

Department of Nuclear Medicine

University of Heidelberg

Im NeuenheimerFeld 400

69120 Heidelberg

Tel. +49-6221-56-37164 (Fax. +49-6221-56-5473)

Email: clemens.kratochwil@med.uni-heidelberg.de

Running Title: PMPA kidney-protection in PSMA therapy

Word count: 4343

Abstract:

Radioactive ligands for the prostate specific membrane antigen (PSMA) are under development for therapy of metastasized prostate cancer (PCa). Since PSMA expression is also found in the kidneys, renal tracer uptake can be dose limiting. As kidney kinetics differs from tumor kinetics, serial application of PSMA-inhibitors such as 2-(phosphonomethyl)pentanedioic acid (PMPA) could improve the kidney-to-tumor ratio. In this study, we evaluate the effect of PMPA on the biodistribution of two promising PSMA-ligands.

Methods: Human PCa xenografts (LNCaP) were transplanted s.c. into mice. After injection of ¹²⁵I-MIP1095, a 16h latency period was given to allow tracer clearance from the blood and renal calices. After baseline scintigraphy PMPA was injected in doses of 0.2-50 mg/kg (n=3 per dose, 5 controls), followed by scans at 2h, 4h, 6h and 24h post PMPA injection. Kidney and tumor displacement was determined as percentage of baseline. A shortened but similar design was used to evaluate the PSMA ligand MIP1404 which contains a chelate for ^{99m}Tc/Re.

Results: PMPA injection 16h after MIP1095 translated into a rapid and quantitative relevant displacement of renal activity. The tumor uptake was reduced to a significant lesser extent also in a dose dependent manner. PMPA doses of 0.2-1mg/kg appear optimal to sustain nearly complete tumor uptake while simultaneously achieving near total blocking of specific renal PSMA-binding. The effect was successfully validated with the PSMA ligand MIP1404.

Conclusion: PSMA targeted radionuclide therapy can benefit from serial PMPA co-medication by reducing off-target radiation to kidneys. These data will be used for a first approximation in clinical translation, although in patients an optimization of the dose and time schedule may be necessary.

Keywords: PSMA, PMPA, prostate cancer, radionuclide therapy, nephroprotection

INTRODUCTION

Intense overexpression of the cell surface peptidase prostate-specific membrane antigen (PSMA) in the majority of both primary and metastatic prostate cancers (PCa) as well as a positive correlation of PSMA with traditional adverse prognostic factors aroused growing interest in evaluation of this target (1-3). Initially, antibodies (mAb) targeting PSMA have been used for PCa imaging and therapeutic approaches. The ^{111}In labeled mAb capromab (ProstaScint, EUSA Pharma, Oxford, England) targeted to a cytoplasmic domain of PSMA was even approved in the USA. However the diagnostic value of intracellular targeting was rather limited (4). The mAb J591 targets the extracellular domain of PSMA, but like most full-length mABs it is characterized by a slow tumor accumulation and a long circulation time in blood. Thus diagnostic mAB-tracers require prolonged imaging - even days after injection (5). In the context of radionuclide therapy mABs commonly translate into an unfavorable dosimetry with pronounced hematotoxicity (6). Recently, the development of the Glu-urea-based high affinity small molecule PSMA inhibitors MIP1072 and MIP1095, either labeled with ^{123}I for imaging or ^{131}I for targeted radionuclide therapy, rendered rapid tumor uptake possible (7-9). Since PSMA is internalized through clathrin-coated pits (10) either spontaneously or after binding of an antibody or an inhibitor it is also an excellent target for systemic radionuclide therapy. In this respect the accumulation of the tracer in normal tissues has to be considered to prevent or diminish the extent of side effects. In a positron emission tomography (PET)-based dosimetry study of ^{124}I -MIP1095 in patients with castration refractory prostate cancer (CRPCa), doses of up to 300Gy in lymph node and bone metastases were assessed. The organs with the highest off-target radiation doses were salivary glands (3.8 mSv/MBq), liver (1.7 mSv/MBq) and kidneys (1.4 mSv/MBq); red marrow was 0.37 mSv/MBq (11). A 23 Gy tolerance limit was suggested for kidneys during conventional radiotherapy (12) and the biological effective dose (BED) in systemic radionuclide therapy, which depends on the half-life of the used radionuclide, can markedly vary in both directions (13). Therefore, kidneys might be the limiting factor for the maximum activity that can cumulative be administered safely. However, minimizing kidney uptake without losing tumor dose is a real challenge because PSMA is physiologically expressed in the kidney tubules (1). The pharmacokinetics of MIP1072 vs MIP1095 in animals have already been evaluated in detail (7,14). The authors reported a similar accumulation of both compounds in PSMA-expressing LNCaP xenografts but with very different pharmacokinetic profiles. MIP1072 clears rapidly from target and non-target tissues. In contrast MIP1095 presents a longer biological half-life in tumor

but not in kidneys, which corresponds to a higher fraction of ligand induced receptor internalization in tumor cells.

For the development of PSMA ligands the structurally unrelated PSMA inhibitor 2-(phosphonomethyl)pentanedioic acid (PMPA) is commonly used as a competitor in blocking studies to demonstrate the specific binding of the molecule of interest. In this respect simultaneous coinjection of 50mg/kg PMPA resulted in a complete blocking of MIP1095 binding sites in tumor and kidneys (7).

The thesis for the actual study is, that after internalization of Glu-urea-based radiolabeled PSMA-ligands into the tumor cells, a subsequent administration of high dose PSMA-competitor PMPA might no longer block tumor uptake but could still displace the “non” or “not yet” internalized PSMA-ligand from the renal tubular cells, thus improving the projected tumor-to-kidney dose ratio.

MATERIALS AND METHODS

Inoculation of Mice with LNCaP Xenografts

All animal studies were approved by the Institutional Animal Care and Use Committee in accordance with the guidelines for Care and Use of Laboratory Animals. Mice were housed under standard conditions in approved facilities with 12-h light/dark cycles and given food and water ad libitum. BALB/c nude mice were implanted with 5×10^6 LNCaP cells (BD Biosciences) suspended in Matrigel (BD Biosciences) behind the left shoulder. The mice were used for our study after 8-12 weeks, when the tumors reached approximately 1.5 cm in diameter.

Radiolabeling of MIP1095 and MIP1404

The synthesis of MIP1095 (S)-2-(3-((S)-1-carboxy-5-(3-(4-iodophenyl)ureido)pentyl)ureido)pentanedioic acid, the radiolabeling precursor trimethyltin-MIP-1095 and the subsequent radiolabeling with a variety of iodine isotopes was described previously (14,15). MIP1404 was provided from Molecular Insight Pharmaceuticals (Cambridge, USA) and labeled with ^{99m}Tc eluted from a clinical approved generator (ELUMATIC III, IBA, Belgium). The synthesis of MIP1404 has also been described previously (16).

Workflow of MIP-1095 and MIP-1404 Animal Studies

Mice bearing LNCaP tumors of 1.5 cm diameter were injected via the tail vein with 37 MBq of ^{125}I -MIP1095 in 100 μl at a specific activity of $>1,000$ mCi/Amol. Mice were imaged at 16 h post injection (baseline) giving enough time for tumor uptake and internalization and tracer clearance from the blood stream and kidney calices. Immediately after the baseline scan PMPA in 100 μl physiological saline solution was injected via the tail vein in doses of 50mg/kg, 10mg/kg, 1mg/kg, 0.2 mg/kg (n=3 per dose) or the animals served as controls (n=5). Planar scans were performed 2h, 4h, 6h and 24h post PMPA injection (see also chart **Fig. 1A**).

MIP1404 was evaluated after labeling with $^{99\text{m}}\text{Tc}$ in LNCaP bearing BALB/c nude mice. The baseline scintigraphy was done 1h after injection of 9.3 - 11 MBq $^{99\text{m}}\text{Tc}$ -MIP1404 in 100 μl directly followed with the injection of 50 mg/kg PMPA in 50 μl or 50 μl saline (n=3, respectively). Planar scans were done 1h and 3h after the sub-sequent PMPA/saline injection. The flow chart of the experiment is presented in **Fig. 2A**. Quantification was done with kidney ROIs arising counts per minute (cpm) which were then converted to percentage-of-baseline values. The same protocol was used to evaluate kidney uptake of 10.3-11.6 MBq $^{99\text{m}}\text{Tc}$ -MIP1404 in 100 μl directly followed with the injection of 50 mg/kg, 10 mg/kg and 1 mg/kg PMPA in 50 μl or saline as controls (n=4, respectively) in non-tumor bearing NMRI mice (**Supplement-Fig. 1A**). In a pilot experiment planar scans after injection of the salivary gland tracer $^{99\text{m}}\text{Tc}$ pertechnetate were acquired and the diagnostic value of the images was judged visually.

Technique of Small Animal Scintigraphy

During imaging mice were anesthetized using 1% isoflurane gas in oxygen flowing at 0.6 L/min. Serial planar scans were done with a Gamma Imager-sct (biospace labs, Paris, France). Quantification of tumor and kidney uptake was done by determining the cpm in the target region by ROI-technique. The baseline scan before administration of PMPA served as reference, the subsequent images are reported as percentage of the baseline value. PET scans were performed using a dedicated small animal PET scanner (Siemens, Inveon) and quantification was done by VOI-technique and reported as standardized uptake values (SUV).

RESULTS

MIP1095

Subsequent injection of PMPA 16h after MIP1095 translated into a rapid and quantitatively significant displacement of renal activity for all PMPA doses tested. Scintigraphy scans from one example out of each group are presented in **Fig. 1B**. The course of residual activity of ¹²⁵I-MIP1095 measured at the particular time points after subsequent administration of 0.2mg/kg, 1mg/kg, 10mg/kg, 50mg/kg PMPA or controls are presented in **Fig. 3A** for kidney and **Fig. 3B** for tumor ROIs. Even at a very low dose of 0.2 mg/kg, there is a high significant ($p<0.01$) displacement from the kidneys. The effect was more pronounced at higher doses and showed a dose dependency with 1mg/kg revealing an even higher kidney wash-out than the 0.2 mg/kg dose ($p<0.01$). However, doses >1 mg/kg did not result in further improvement of the kidney protective effect (differences between 1mg/kg, 10mg/kg and 50mg/kg PMPA groups were non-significant). In tumor tissue, the uptake of ¹²⁵I-MIP1095 was displaced by subsequent injection of PMPA and this effect appeared to be dose dependent: residual uptake 2h after PMPA was 98% with 0.2 mg/kg, 93% with 1 mg/kg, 77% with 10 mg/kg and 75 % with 50 mg/kg. However, due to the small size of the group ($n=3$) none of the differences was statistically significant.

MIP1404

Normalized to the 1h p.i. tumor uptake there is a fast wash-out of MIP1404 from the kidneys even without intervention. When 50mg/kg PMPA were administered directly following the baseline scan the wash-out was significantly ($p<0.01$) enhanced at time point 2h and 4h (**Fig. 2B, Fig. 4A**). Comparing to controls, the difference in tumor uptake measured in the PMPA group was non-significant already with the 50mg/kg PMPA dose (**Fig. 4B**). As MIP1404 seemed rather robust against tumor displacement even after high dose PMPA the dilution series with 50mg/kg, 10mg/kg, 1mg/kg and saline were done in non-tumor bearing NMRI mice. Residual kidney uptake at time point 2h and 4h were 36 % and 15% in controls, 13% and 9% after 1mg/kg PMPA, 15 and 10 % after 10 mg/kg PMPA, 11% and 7% after 50 mg/kg PMPA (**Supplement-Fig. 1B**). This pattern is consistent with the larger MIP1095 series, demonstrating optimal kidney displacement even at 1mg/kg and no benefit of higher PMPA doses. In a pilot study planar scans of the mice were acquired after injection of ^{99m}Tc pertechnetate which is known to accumulate in the salivary glands but due to the limited spatial resolution of the camera we were not able to sufficiently delineate these small structures in mice (**Supplement-**

Fig. 2). Thus, we concluded that it is not feasible to further evaluate a potential displacement of MIP1404 out of the salivary glands with this study design.

DISCUSSION

PSMA is an emerging target for imaging and radionuclide therapy of metastasized PCa. In regard to radionuclide therapy MIP1095, MIP1404 are promising PSMA-ligands, because these small molecules enable fast tumor targeting, present fast clearance from un-targeted organs and warrant sufficient residency times in tumor due to ligand induced cellular internalization (7,11). MIP1404 is of particular interest because its single amino acid chelator (SAAC) can be either labeled with diagnostic ^{99m}Tc or in therapeutic intention with ^{186}Re or ^{188}Re (16,17). Technetium and rhenium are chemically related and share structural as well as reactive similarities. ^{99m}Tc is available from approved generator systems and can be imaged with the numerous already installed angler cameras. ^{186}Re (half-life 3.7 days, max. energy of beta-emission 1.07 MeV, 11% co-emission of 137 keV gammas for imaging) presents an attractive “matched pair” for therapy. ^{188}Re (half-life 17h, max. energy of beta-emission 2.12 MeV, 15% co-emission of 155 keV gammas for imaging) can be obtained from a $^{188}\text{W}/^{188}\text{Re}$ generator system (Oak Ridge National Laboratory) which was FDA approved and would be suitable for clinical application (18). MIP1095 can be tagged with different isotopes of iodine. Until now, most of the clinical experience is available for this compound. Labeled with ^{124}I it was already used for PET-based dosimetry and labeled with ^{131}I in therapy of patients with treatment-refractory advanced prostate cancer (11). For human beings ^{123}I offers good imaging probabilities (159 keV gamma emission, 12h half-life) for conventional scintigraphy (7). Labeled with ^{125}I (half-life 60 days, gamma emission 27-35 keV) it presents the best characteristics for small animal imaging and therefore ^{125}I -MIP1095 was chosen for our main experiment.

After the subsequent injection of PMPA a relevant kidney displacement was observed with both radiotracers regardless of whether the evaluated compound included a chelate (MIP1404) or not (MIP1095). Thus, in addition to some nonspecific kidney uptake due to tubular reabsorption - which might be further improved by modifications affecting the chelate or linker of the tracer molecule - a relevant part of kidney uptake seems to be related to specific PSMA binding.

It is common practice to show specific binding of PSMA ligands by simultaneous co-injection of 50mg/kg PMPA which results in a complete blocking of PSMA binding sites in tumor and

kidneys (7,14,16). Our findings now implicate that a subsequent injection of this competitor cannot displace the endosome-fixed ligand from the tumor; by contrast, it can still displace the non-internalized ligands from the kidneys.

PSMA was found to be equal to the enzyme glutamate carboxypeptidase II (GCPII) and today both terms are used as synonyms. Immunostaining revealed a physiologic expression of PSMA in the kidney tubules already in 1997 (1). However, glutamate carboxypeptidase III (GCPIII), a GCP II homolog with 67% amino acid identity, was cloned and evaluated on RNA level in 2007, but lacking a GCP III specific antibody different amounts of GCP II and III on the cell surface of different tissues cannot be assessed on protein level until now (19). A third enzyme with high similarity to GCP II is NAALADase L (20). Therefore, it is possible that the PSMA expressed by the renal tubular cells simply represents a different isoform of the molecule with a lower internalization rate.

However, even if the kidney expresses GCP II there are potentially other mechanisms that could account for the different tracer kinetics. It was reported that binding of PSMA to filamin A reduces its internalization rate by 50% (21). Glycosylation can also regulate GCP II enzyme activity via redistribution of the protein from the plasma membrane to intracellular loci, as well as by affecting its half-life (22). Furthermore, the sensitivity of PSMA to treatment with different glycosidases was different in different prostate carcinoma cell lines indicating that these may be composed of different types of sugar structures (23). Thus, a different expression of PSMA co-factors or different glycosylation patterns in kidney and tumor would also be a sufficient explanation for our observations.

Nevertheless, preclinical animal studies are associated with some limitations. In our study design, the PSMA expressed by the LNCaP xenografts present the human form of GCP II, the kidney PSMA presents the ortholog of mice. Rovenska et al characterized human PSMA with its rat and pig orthologs and found the GCP II of these species suitable to approximate human GCP II enzyme activity (24). However, variants of PSMA among different species should always be considered when using animal models and might complicate the extrapolation of preclinical observations to clinical application.

The salivary glands present another organ with a high uptake of diagnostic PSMA-tracers (8) and also to ¹³¹I-MIP1095 which vice versa was found to translate into xerostomia as a side effect in PSMA targeted radionuclide therapy (11). Different reports exist concerning PSMA expression in salivary glands. Silver (1) and Mhaweck-Fauceglia (25) found no expression in

the parotids. However, PSMA RNA has been found in salivary glands (26), in tissue extracts (27) and finally also by immunohistochemistry (28). A variety of mABs binding to different epitopes of the extracellular domain of PSMA presented with different stainings of normal tissues (28), which might be interpreted as another indicator that different splicing variants of PSMA may exist. However, the three antibodies evaluated in the cited study showed no binding to the kidneys which raises some doubts about the reliability of the used antibodies in regard to their specificity and binding affinity. Therefore, the situation in salivary glands is rather unclear. If PSMA expression is responsible for tracer accumulation in the salivary glands PMPA could also be suitable to displace radioactive PSMA ligands from these organs. However, in our small animal imaging experiments no sufficient delineation of this target structure was possible - not even in explicit salivary gland scintigraphy with ^{99m}Tc -pertechnetate. Therefore, we cannot draw a conclusion if PMPA is also suitable to decrease the risk of xerostomia as a potential side effect of PSMA targeted radionuclide therapy at present.

With regard to kidneys, the optimal dose of PMPA was found to be in the range of 0.2-1.0 mg/kg. 1.0 mg/kg translates into near total renal displacement with only minimal (<10%) effect on tumor uptake. With 0.2 mg/kg the decrease in tumor uptake was <5%, but still a relevant improvement of kidney uptake could be observed. Nevertheless, renal activity was only sub-totally displaced with the lower dose. Doing a conservative, body surface based, extrapolation from the 0.2 mg/kg mouse dose to men, an 80kg patient should receive about 60mg of PMPA.

The orally bioavailable PSMA-inhibitor 2-(3-mercaptopropyl)pentanedioic acid (2-MPPA) which is nearly as potent as 2-(phosphonomethyl)pentanedioic acid (2-PMPA) – IC_{50} 85 nM vs. 30 nM (29,30) – was already evaluated in 25 healthy subjects with a mean body weight of 71 kg. Doses of up to 750 mg (i.e. ~10 mg/kg) were found safe and generally well tolerated (31). This presents an approximately 10-fold safety factor in comparison to our recommended starting dose for the evaluation of PMPA based kidney protection during PSMA targeted radionuclide therapy in men. In animal studies even much higher doses of PMPA have also been found tolerable (32). Preliminary data also suggest that selective PSMA-inhibitors such as 2-MPPA or 2-PMPA may have inherent anti-cancer potential against PCa and might simultaneously attenuate docetaxel-induced neuropathy (33).

It is difficult to predict how the displacement effect observed in this investigation will translate into kidney dose of PCa patients because the metabolic turnover of PSMA-inhibitors is much faster in rodents than in human beings. The biological half-life of MIP1095 in the mice kidney of

our control group was approximately 6h (Fig. 3A). In contrast, it was 60-72h in patients evaluated with ^{124}I -MIP1095 (11). Therefore it is not reasonable to simulate the dosimetry effect in men based on the currently available data, yet. Further studies are needed to quantify the kidney dose reduction that can actually be achieved with the presented concept in clinical application.

CONCLUSION

Our data originally demonstrate that it is possible to lower the dose limiting kidney uptake in PSMA-targeted radionuclide therapy with the subsequent injection of the small molecule PSMA inhibitor PMPA without significantly diminishing tumor uptake and retention.

Taking into account the potential benefits versus the residual risks for the unapproved administration of PMPA we consider it ethically reasonable to offer subsequent PMPA co-medication as a kidney protective during PSMA targeted radionuclide therapy. However, further studies are required to optimize the time schedule for the subsequent application of PMPA after radiolabeled PSMA ligands and for the extrapolation from animal to human beings.

Acknowledgement:

This study was initially supported by Molecular Insight Pharmaceutical, Inc., later by Progenics Pharmaceuticals Inc. - in providing the precursors of MIP1095 and MIP1404, respectively.

We also thank Ursula Schierbaum for her help in inoculation of the LNCaP xenografts and Susanne Kraemer for execution of the radiolabeling process.

Disclosure:

The authors declare that they have no conflict of interest.

References:

1. Silver DA, Pellicer I, Fair WR, Heston WD, Cordon-Cardo C. Prostate-specific membrane antigen expression in normal and malignant human tissues. *Clin Cancer Res.* 1997;3:81-85.
2. Ross JS, Sheehan CE, Fisher HA, et al. Correlation of primary tumor prostate-specific membrane antigen expression with disease recurrence in prostate cancer. *Clin Cancer Res.* 2003;9:6357-6362.
3. Eder M, Eisenhut M, Babich J, Haberkorn U. PSMA as a target for radiolabelled small molecules. *Eur J Nucl Med Mol Imaging.* 2013;40:819-823.
4. Rosenthal SA, Haseman MK, Polascik TJ. Utility of capromab pendetide (ProstaScint) imaging in the management of prostate cancer. *Tech Urol.* 2001; 7:27-37.
5. Vallabhajosula S, Kuji I, Hamacher KA, et al. Pharmacokinetics and biodistribution of ¹¹¹In and ¹⁷⁷Lu labeled J591 antibody specific to prostate specific membrane antigen: prediction of ⁹⁰Y-J591 radiation dosimetry based on ¹¹¹In or ¹⁷⁷Lu. *J Nucl Med.* 2005;46:634-641.
6. Tagawa ST, Milowsky MI, Morris M, et al. Phase II study of Lutetium-177-labeled anti-prostate-specific membrane antigen monoclonal antibody J591 for metastatic castration-resistant prostate cancer. *Clin Cancer Res.* 2013;19:5182-5191.
7. Barrett JA, Coleman RE, Goldsmith SJ, et al. First-in-man evaluation of 2 high-affinity PSMA-avid small molecules for imaging prostate cancer. *J Nucl Med.* 2013;54:380-387.
8. Afshar-Oromieh A, Malcher A, Eder M, et al. PET imaging with a [⁶⁸Ga]gallium-labelled PSMA ligand for the diagnosis of prostate cancer: biodistribution in humans and first evaluation of tumour lesions. *Eur J Nucl Med Mol Imaging.* 2013;40:486-495.
9. Afshar-Oromieh A, Zechmann CM, Malcher A, et al. Comparison of PET imaging with a (⁶⁸Ga)-labelled PSMA ligand and (¹⁸F)-choline-based PET/CT for the diagnosis of recurrent prostate cancer. *Eur J Nucl Med Mol Imaging.* 2014;41:11-20.
10. Liu H, Rajasekaran AK, Moy P, et al. Constitutive and antibody-induced internalization of prostate-specific membrane antigen. *Cancer Res.* 1998;58:4055-4060.

11. Zechmann CM, Afshar-Oromieh A, Armor T, et al. Radiation dosimetry and first therapy results with a ¹²⁴I/ ¹³¹I-labeled small molecule (MIP-1095) targeting PSMA for prostate cancer therapy. *Eur J Nucl Med Mol Imaging*. 2014;41:1280-1292.
12. Emami B, Lyman J, Brown A, et al. Tolerance of normal tissue to therapeutic irradiation. *Int J Radiat Oncol Biol Phys*. 1991;21:109-122.
13. Oehme L, Doerr W, Wust P, Kotzerke J. Influence of time-dose-relationships in therapeutic nuclear medicine applications on biological effectiveness of irradiation: consequences for dosimetry. *Nuklearmedizin*. 2008;47:205-209.
14. Hillier SM, Maresca KP, Femia FJ, et al. Preclinical evaluation of novel glutamate-urea-lysine analogues that target prostate-specific membrane antigen as molecular imaging pharmaceuticals for prostate cancer. *Cancer Res*. 2009;69:6932-6940.
15. Maresca KP, Hillier SM, Femia FJ, et al. A series of halogenated heterodimeric inhibitors of prostate specific membrane antigen (PSMA) as radiolabeled probes for targeting prostate cancer. *J Med Chem*. 2009;52:347-357.
16. Hillier SM, Maresca KP, Lu G, et al. ^{99m}Tc-labeled small-molecule inhibitors of prostate-specific membrane antigen for molecular imaging of prostate cancer. *J Nucl Med*. 2013;54:1369-1376.
17. Lu G, Maresca KP, Hillier SM, et al. Synthesis and SAR of ^{99m}Tc/Re-labeled small molecule prostate specific membrane antigen inhibitors with novel polar chelates. *Bioorg Med Chem Lett*. 2013;23:1557-1563.
18. Argyrou M, Valassi A, Andreou M, Lyra M. Rhenium-188 production in hospitals, by w-188/re-188 generator, for easy use in radionuclide therapy. *Int J Mol Imaging*. 2013:290750.
19. Hloučková K, Barinka C, Klusák V, et al. Biochemical characterization of human glutamate carboxypeptidase III. *J Neurochem*. 2007;101:682-696.
20. Pangalos MN, Neefs JM, Somers M, et al. Isolation and expression of novel human glutamate carboxypeptidases with N-acetylated α -linked acidic dipeptidase and dipeptidyl peptidase IV activity. *J Biol Chem*. 1999;274:8470-8483.

21. Anilkumar G, Rajasekaran SA, Wang S, Hankinson O, Bander NH, Rajasekaran AK. Prostate-specific membrane antigen association with filamin A modulates its internalization and NAALADase activity. *Cancer Res.* 2003;63:2645-2648.
22. Barinka C, Rinnova M, Sacha P, et al. Substrate specificity, inhibition and enzymological analysis of recombinant human glutamate carboxypeptidase II. *J Neurochem.* 2002;80:477-487.
23. Ghosh A, Heston WDW. Effect of carbohydrate moieties on the folate hydrolysis activity of the prostate specific membrane antigen. *Prostate.* 2003;57:140-151.
24. Rovenská M, Hloučová K, Sácha P, et al. Tissue expression and enzymologic characterization of human prostate specific membrane antigen and its rat and pig orthologs. *Prostate.* 2008;68:171-182.
25. Mhaweck-Fauceglia P, Zhang S, Terracciano L, et al. Prostate-specific membrane antigen (PSMA) protein expression in normal and neoplastic tissues and its sensitivity and specificity in prostate adenocarcinoma: an immunohistochemical study using multiple tumour tissue microarray technique. *Histopathology.* 2007;50:472-483.
26. Israeli RS, Powell CT, Corr JG, Fair WR, Heston WD. Expression of the prostate-specific membrane antigen. *Cancer Res.* 1994;54:1807-1811.
27. Troyer JK, Beckett ML, Wright GLJr. Detection and characterization of the prostate-specific membrane antigen (PSMA) in tissue extracts and body fluids. *Int J Cancer.* 1995;62:552-558.
28. Wolf P, Freudenberg N, Bühler P, et al. Three conformational antibodies specific for different PSMA epitopes are promising diagnostic and therapeutic tools for prostate cancer. *Prostate.* 2010;70:562-569.
29. Jackson PF, Tays KL, Maclin KM, et al. Design and pharmacological activity of phosphinic acid based NAALADase inhibitors. *J Med Chem.* 2001;44:4170-4175.
30. Tsukamoto T, Majer P, Vitharana D, et al. Enantiospecificity of glutamate carboxypeptidase II inhibition. *J Med Chem.* 2005;48:2319-2324.

31. van der Post JP, de Visser SJ, de Kam ML, et al. The central nervous system effects, pharmacokinetics and safety of the NAALADase-inhibitor GPI 5693. *Br J Clin Pharmacol.* 2005;60:128-136.
32. Chen SR, Wozniak KM, Slusher BS, Pan HL. Effect of 2-(phosphono-methyl)-pentanedioic acid on allodynia and afferent ectopic discharges in a rat model of neuropathic pain. *J Pharmacol Exp Ther.* 2002;300:662-667.
33. She Y, Tang Z, Lapidus RG, Wozniak KM, Scher HI, Slusher BS. 2-MPPA, a selective inhibitor of PSMA, delays prostate cancer growth and attenuates taxol-induced neuropathy in mice. *J Clin Oncol.* 2005;16S:8054.

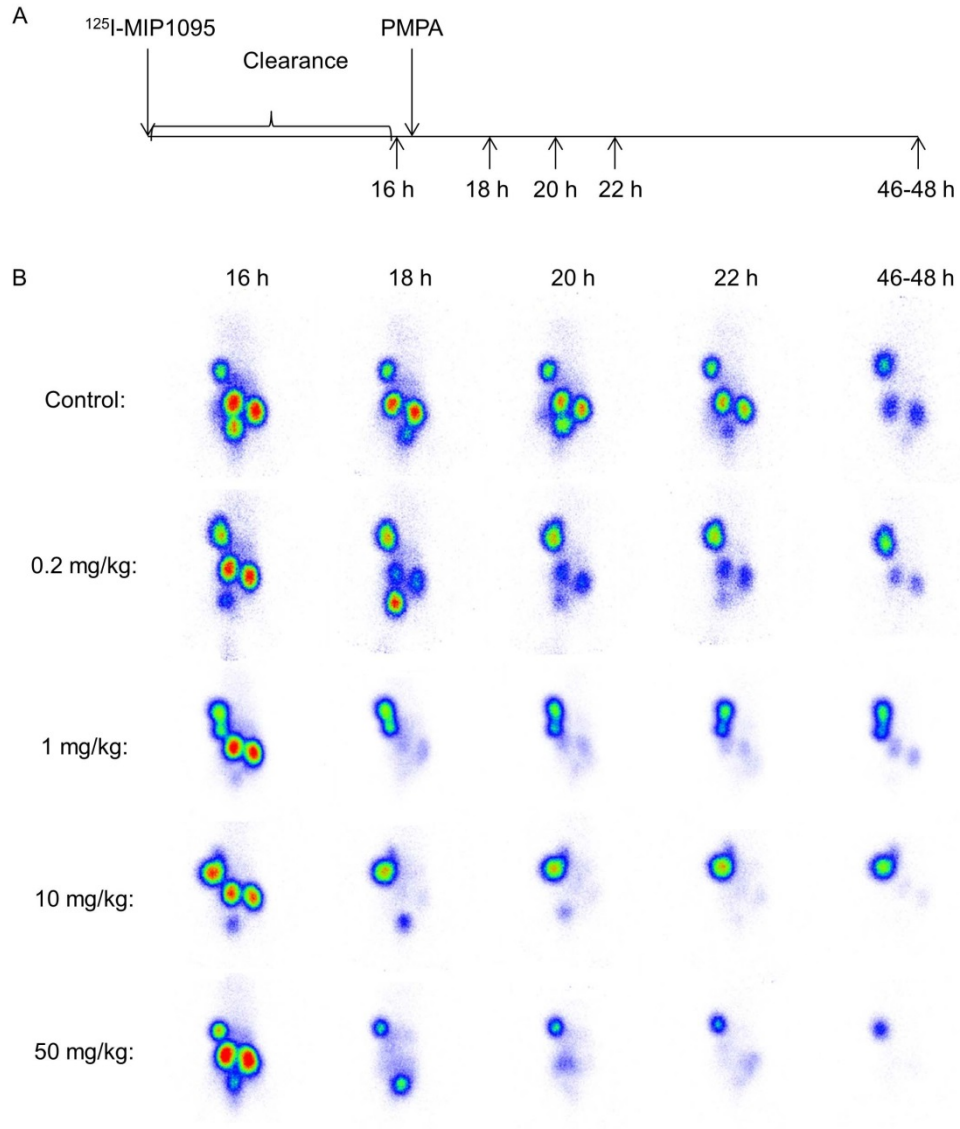


FIGURE 1: Chart demonstrating the experimental setup with the first image at 16 h p.i.. Immediately after scintigraphy saline (control group) or different doses of PMPA were given and additional imaging was done at the indicated time periods p.i. (A). One example image of controls and each PMPA group, respectively (B).

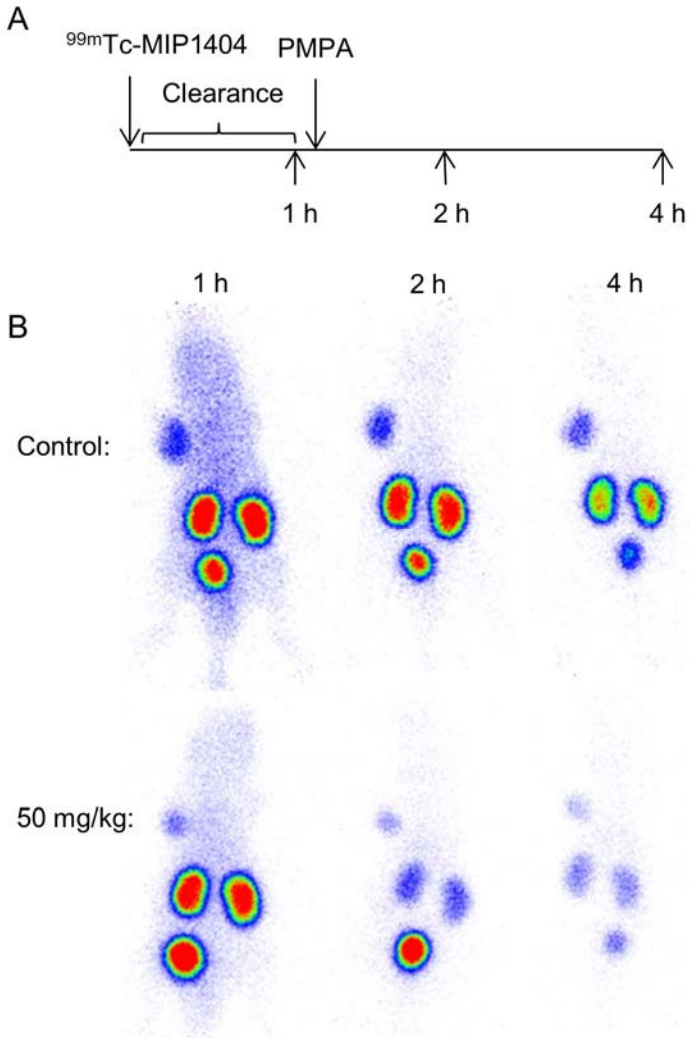


FIGURE 2: Chart demonstrating the experimental setup with the first image at 1 h p.i.. Immediately after scintigraphy saline (control group) or 50mg/kg PMPA were given and additional imaging was done at the indicated time periods p.i. (A). Scintigraphic images of a control and a PMPA treated animal (B).

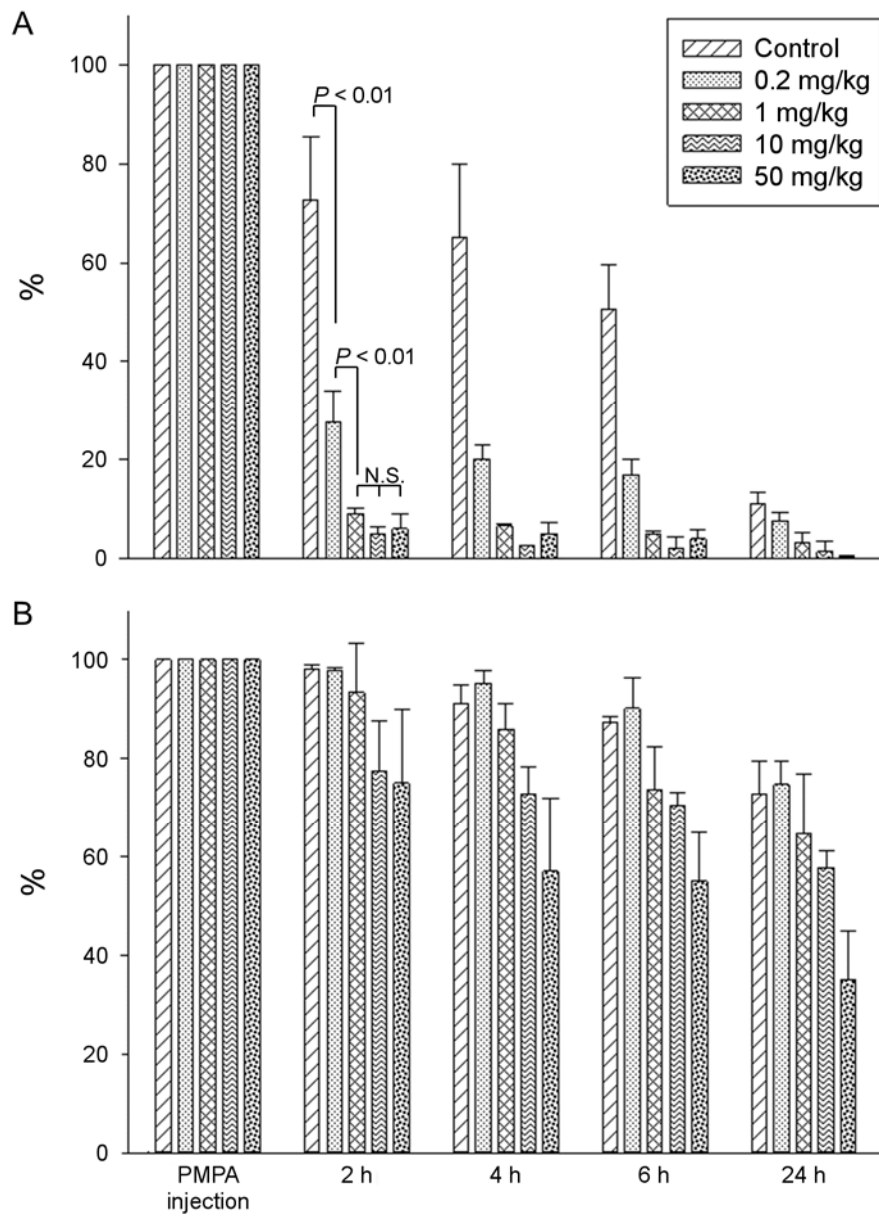


FIGURE 3: Time course of residual activity in the kidney (A) and tumor (B) expressed in % of the value at PMPA or saline injection.

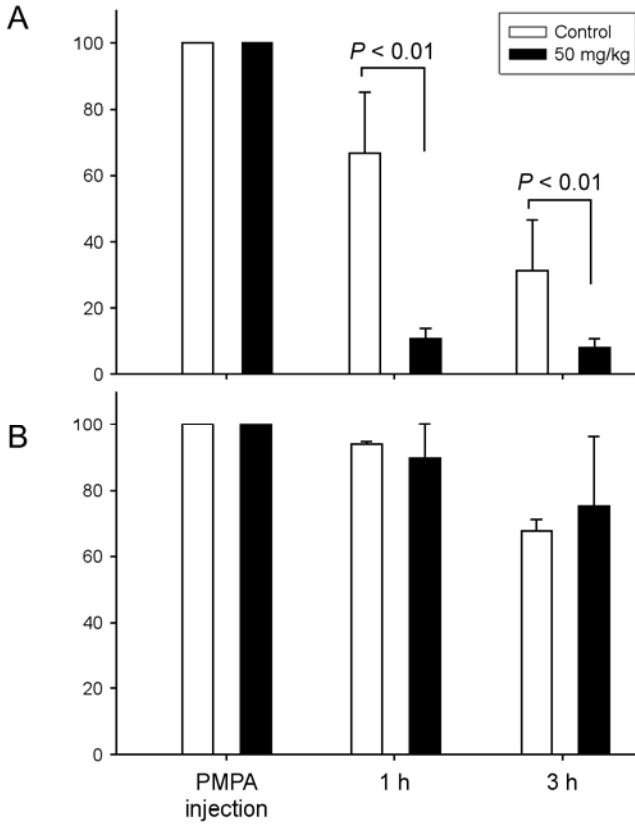


FIGURE 4: Time course of residual activity in the kidney (A) and tumor (B) expressed in % of the value at PMPA or saline injection.